An Equilibrium Model for the Mg2+−Linked Self-Assembly of FtsZ in the Presence of GTP or a GTP Analogue

ARTICLE *in* BIOCHEMISTRY · JULY 2012

Impact Factor: 3.02 · DOI: 10.1021/bi300891q · Source: PubMed

3 AUTHORS:

Begoña Monterroso
Spanish National Research Council
24 PUBLICATIONS **421** CITATIONS
SEE PROFILE

Germán Rivas
Spanish National Research Council
101 PUBLICATIONS **2,675** CITATIONS
SEE PROFILE

Allen P Minton
National Institutes of Health
169 PUBLICATIONS **10,773** CITATIONS
SEE PROFILE

Published in final edited form as:
Biochemistry. 2012 August 7; 51(31): 6108–6113. doi:10.1021/bi300891q.

An Equilibrium Model for the Mg^{2+}-Linked Self-Assembly of FtsZ in the Presence of GTP or a GTP Analogue

Begoña Monterroso[†], **Germán Rivas**[*,†], and **Allen P. Minton**[*,‡]

[†]Chemical and Physical Biology Program, Centro de Investigaciones Biológicas, Consejo Superior de Investigaciones Científicas, Madrid, Spain

[‡]Section on Physical Biochemistry, Laboratory of Biochemistry and Genetics, National Institute of Diabetes and Digestive and Kidney Diseases, National Institutes of Health, Bethesda, Maryland 20892, United States

Abstract

The concerted formation of a narrow distribution of oligomeric FtsZ species in the presence of GTP or a GTP analogue under close to physiological conditions (neutral pH and 0.5 M K^+) has been characterized recently by various biophysical methods [Monterroso, B., et al. (2012) *Biochemistry 51*, 4541–4550]. An equilibrium model may semiquantitatively account for the results of this study; in the model, FtsZ self-associates in a noncooperative fashion to form linear fibrils, that upon increasing to a certain size exhibit an increasing tendency to form closed cyclic fibrils, as previously suggested [González, J. M., et al. (2005) *Proc. Natl. Acad. Sci. U.S.A. 102*, 1895–1900]. The closed cyclic fibrils are formed when the natural curvature and flexibility of a linear oligomer bring the ends of a linear fiber sufficiently close to overcome the entropic barrier to loop closure. The size distribution of cyclic oligomers is thus a reflection of the tendency toward curvature of linear fibrils of FtsZ under the conditions used in these experiments.

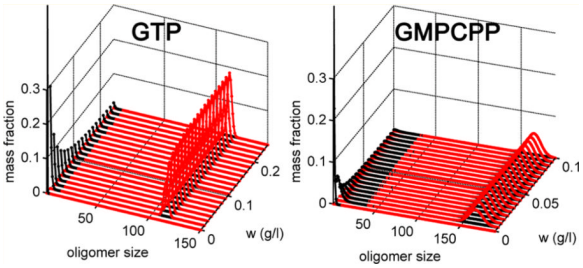

We have recently characterized the Mg^{2+}- and concentration-dependent self-assembly of FtsZ in the presence of GTP and GMPCPP, a slowly hydrolyzable analogue of GTP, by a variety of thermodynamic and hydrodynamic techniques, including static light scattering, sedimentation velocity, fluorescence correlation spectroscopy, and dynamic light scattering.[1] We have found that as the protein concentration increases in the presence of either of these

[*]**Corresponding Author**: G.R.: grivas@cib.csic.es; phone, + 34 918373112. A.P.M.: minton@helix.nih.gov; phone, (301) 496-3604.

ASSOCIATED CONTENT

Supporting Information

Dependence of i_{max} with α for the FtsZ solutions in GTP/RS with 100 μM Mg, GTP/RS with 5 mM Mg, and GMPCPP with 5 mM Mg (Figure S1) and electron microscopy images of FtsZ polymerized with GTP and GMPCPP (Figure S2). This material is available free of charge via the Internet at http://pubs.acs.org.

Notes

The authors declare no competing financial interest.

cofactors, FtsZ undergoes a concerted transition between a paucidisperse distribution of low-molecular weight species (monomer, dimer, and trimer) and a narrow size distribution of high-molecular weight species containing of the order of 80–120 protomers in the presence of GTP and 140–180 protomers in the presence of GMPCPP. Although the peak size of the distribution varies with nucleotide type and magnesium concentration, the concerted nature of the transition does not. A further increase in protein concentration increases the population of high-molecular weight species but not the mean size or dispersity, suggesting a process thermodynamically equivalent to a second-order phase transition as previously proposed.[2] The purpose of this work is to demonstrate that a relatively simple equilibrium model can quantitatively account for all of the data presented in the study cited above.

Several authors[3–6] have proposed an alternate mechanism to account for the cooperative formation of linear FtsZ oligomers. According to this model, the free energy cost of forming a dimer exceeds that required to elongate the fiber beyond a dimer, because of the requirement that both reactant molecules undergo a conformational change upon formation of a dimer, while elongation requires a conformational change on the part of only one reactant (the monomer to be added to the growing oligomer). We refer to this model as the dimer-nucleated isodesmic growth model. In the following section, we introduce a hybrid model that combines the previously proposed dimer nucleation and the isodesmic growth–cyclization model proposed previously by González et al.[2] Via the adjustment of the values of model parameters, the hybrid model can be reduced to either the pure dimer-nucleated isodesmic growth model or the pure isodesmic–cyclization model. In subsequent sections, we show that all of the experimental data presented previously[1] may be explained within experimental uncertainty without inclusion of dimer nucleation.

METHODS

Nucleated Isodesmic Growth–Cyclization Model

We assume, in accordance with ref 3, that the equilibrium constant for formation of dimer is smaller by a factor α than the equilibrium constant for further stepwise growth of a linear fibril:

$$A+A \overset{\alpha K}{\rightleftarrows} A_2 \quad (1)$$

$$\begin{aligned} A_2+A &\overset{K}{\rightleftarrows} A_3 \\ &\cdots \\ A_{i-1}+A &\overset{K}{\rightleftarrows} A_i \end{aligned} \quad (2)$$

We also assume in accordance with ref 2 that a linear fibril may form a cyclic fibril with a length-dependent equilibrium constant

$$A_i \overset{K_i^c}{\rightleftarrows} A_i^c \quad (3)$$

where

$$K_i^c = K_{\max}^c \exp\left[-\left(\frac{i-i_{\max}}{\sigma_c}\right)^2\right] \quad (4)$$

According to this scheme, the concentration of each species of linear oligomer is given by

$$\begin{aligned} c_2 &= \alpha K c_1^2 \\ c_3 &= \alpha K^2 c_1^3 \\ &\cdots \\ c_i &= \alpha K^{i-1} c_1^i \end{aligned} \quad (5)$$

and the concentration of each cyclic oligomer is given by

$$c_i^{(c)} = K_i^c \alpha K^{i-1} c_1^i \quad (6)$$

We define the scaled concentrations

$$\begin{aligned} c_{\text{tot}}^* &= K c_{\text{tot}} \\ c_i^* &= K c_i \end{aligned} \quad (7)$$

It then follows that the total scaled concentration of protomers is given by

$$c_{\text{tot}}^* = \sum_i i[c_i^* + c_i^{(c)*}] = (1-\alpha)c_1^* + \frac{\alpha c_1^*}{1-c_1^*} + \alpha \sum_i i K_i^c (c_1^*)^i \quad (8)$$

We now define the unitless quantity

$$f_1 = c_1 / c_{\text{tot}} = c_1^* / c_{\text{tot}}^* \quad (9)$$

Which when substituted into eq 8 yields

$$(1-\alpha) f_1 + \frac{\alpha f_1}{(1 - f_1 c_{\text{tot}}^*)^2} + \frac{\alpha}{c_{\text{tot}}^*} \sum_i i K_i^c (f_1 c_{\text{tot}}^*)^i - 1 = 0 \quad (10)$$

Given the values of K, K_{max}^c, i_{max}, α, and σ_c, the values of K_i^c may be calculated according to eq 4, and then eq 10 may be solved numerically for the value of f_1 as a function of c_{tot}, providing that the infinite sum indicated in eq 10 is calculated to convergence. Then the concentrations and mass fractions $f_i = ic_i/c_{\text{tot}}$ of all species may be calculated as functions of c_{tot}.

RESULTS

90° Light Scattering Data Analysis

Analysis of the concentration and angle dependence of scattering intensity of FtsZ solutions in GMPCPP and 5 mM Mg was described in ref 1. It was shown that the data could be quantitatively accommodated by a phenomenological first-order phase transition model, according to which a narrow size distribution of high-molecular weight oligomer appears at total concentrations exceeding the solubility. The amount, but not the average size, of high-molecular weight species is postulated to increase almost linearly with the difference between the total concentration and solubility. It was further established that the average size of the oligomer was essentially independent of the concentration of GMPCPP. According to the best fit of the empirical solubility model, the scattering intensity of the high-molecular weight polymer at 0° is estimated to be approximately 3.5 times that at 90°.

As described above, the nucleated isodesmic model may be used to calculate the mass fractions of all species as a function of the total protein concentration. The intensity of scattering measured at 90° is then calculated according to the following generalization of eq 6 in ref 1

$$\frac{R(90^\circ)}{K_{\mathrm{opt}}} \cong M_1 w_{\mathrm{tot}} \left[\sum_i i f_i^{(\mathrm{linear})} + \sum_i i f_i^{(\mathrm{cyclic})} / \Xi \right] + \mathrm{offset} \quad (11)$$

where $f_i^{(\mathrm{linear})}$ and $f_i^{(\mathrm{cyclic})}$ denote the fractional abundances of linear and cyclic $i$mers, respectively, and Ξ denotes the ratio of the intensity of scattering of the high-molecular weight oligomer at 0° to that at 90°. Note that this formulation neglects the correction for scattering of high-molecular weight linear oligomers, but according to the best-fit model, the abundance of these will be negligible. The best fit of this model to the data obtained in the absence and presence of Mg at four concentrations is shown in Figure 1. Best-fit curves at each Mg concentration were calculated using the parameter values listed in Table 1. It is evident that these parameter values cannot be estimated precisely, but several qualitative conclusions may be drawn from the results.

1. The nucleated isodesmic–cyclization model with approximate correction for 90° scattering of large oligomers can fit the data within experimental precision.
2. The stepwise association constant for elongation of a linear fibril increases significantly with an increasing magnesium concentration.
3. It is not necessary to assume that K_2 is substantially smaller than the elongation constant for successive oligomers to account for the appearance of a “critical concentration” associated with the sharp onset of a steep increase in light scattering. However, values of α that are slightly smaller than unity are consistent with these results, as well as results obtained from measurements of multiangle light scattering and measurements of sedimentation velocity and diffusion (see below).
4. The equilibrium constant for conversion of linear to cyclic oligomer cannot be evaluated numerically but is so large that the conversion can be regarded as essentially stoichiometric.
5. If the mean size of the cyclic oligomer is set equal to ~150 in accordance with the value obtained previously using the Svedberg relation,[1] the standard deviation of the assumed normal distribution is on the order of 7–10% of the mean size.

Multiangle Light Scattering Data Analysis

The dependence of scattering intensity upon both protein concentration and scattering angle is given by the following extension of eq 11, which may be compared to eq 7 in ref 1

$$\frac{R(\theta)}{K_{\mathrm{opt}}} \cong M_1 w_{\mathrm{tot}} \left[\sum_i i f_i^{(\mathrm{linear})} + \sum_i i f_i^{(\mathrm{cyclic})} (1 + A_1 g + A_2 g^2) \right] \quad (12)$$

where

$$g = \sin^2(\theta/2)$$

Equation 12, like eq 11, neglects the angular dependence of scattering from large linear oligomers, but it will be shown below that the concentration of such oligomers is expected

to be negligible. Equation 12, with f_i calculated using eqs 4–10, was fit to the dependence of scattering intensity on concentration and scattering angle measured under three sets of conditions: (A) FtsZ with GTP/RS in the presence of 100 μM Mg, (B) FtsZ with GTP/RS in the presence of 5 mM Mg, and (C) FtsZ with GMPCPP in the presence of 5 mM Mg. Each of these sets of data, and the best fit of the nucleated isodesmic–cyclization model to each data set, is plotted in Figure 2A–C. The best-fit parameter values are listed in Table 2. It was observed that the data may be fit equally well over an α range from 0.2 to 1, but the best-fit value of i_{max} depends sensitively upon the fixed value of α. The best-fit value of i_{max} for each data set as a function of the fixed value of α is plotted in Figure S1 of the Supporting Information.

Upon calculating the weight-average molar mass from the nucleated isodesmic–cyclization model, we found that the weight-average degree of polymerization may be significantly less than the value of i_{max}, presumably because of the progressive depletion of longer linear oligomers by the cyclization of shorter oligomers. The concentration-dependent distributions of linear and cyclic oligomers, calculated using eqs 4–11 for each set of experimental conditions using the corresponding set of best-fit parameter values for α = 0.9, are plotted in Figure 3A–C, and the calculated weight-average degrees of polymerization as a function of concentration for each of the three data sets are plotted in Figure 4.

Estimate of the Radius of Gyration of FtsZ Oligomers Formed in 5 mM Mg from Multiangle Light Scattering Data

According to the Zimm–Debye formulation of static light scattering

$$\frac{R}{K_{opt}} = M\left[1 - \left(\frac{R_G{}^2 16\pi^2 n_0{}^2}{3\lambda^2}\right)\sin^2(\theta/2) + \ldots\right] \quad (13)$$

where M is the molar mass, R_G is the radius of gyration, n_0 is the refractive index of solvent, λ is the wavelength of incident light, and θ is the scattering angle.[7] The dependence of the scattering of FtsZ upon protein concentration and scattering angle was shown to be quantitatively described by the following relation:

$$\frac{R(w_{tot}, \theta)}{K_{opt}} = w_{low} M_{w,low} + w_{high} M_{w,high}(1 + A_1 g + A_2 g^2) \quad (14)$$

where w_{low}, w_{high}, $M_{w,low}$, and $M_{w,high}$ are the concentrations and molecular weights of low- and high-molecular weight scatterers, respectively.[1]

Comparison of eqs 13 and 14 gives

$$R_G{}^2 \cong -\frac{3\lambda^2}{16\pi^2 n_0{}^2} A_1 \quad (15)$$

The best fit of eq 14 to the multiangle scattering data obtained for FtsZ polymers in GTP/RS and GMPCPP with 5 mM Mg, shown in Figure 4 of ref 1, yielded the following best-fit values: $M = (4.5 \pm 0.3) \times 10^6$ and $A_1 = -2.05 \pm 0.4$ for GTP-FtsZ, and $M = (6.4 \pm 0.7) \times 10^6$ and $A_1 = -2.37 \pm 0.5$ for GMPCPP-FtsZ. From these values, using an n_0 of 1.333 and a λ of 690 nm, we estimate the radius of gyration of GTP-FtsZ to be 1000 ± 100 Å and that of GMPCPP-FtsZ to be 1100 ± 110 Å.

An upper limit for the radius of gyration of a cyclic oligomer of FtZ may be estimated by assuming that this corresponds to the radius of a planar circle of beads representing FtsZ

monomers. This circle has a circumference approximately equal to n times the diameter of a FtsZ monomer, d, which is approximately 50 Å. Using the average molar masses of oligomers as determined by both static light scattering and combined hydrodynamic measurements, the mean stoichiometry of the oligomer of GTP-FtsZ is estimated to be 100 ± 20 and that of GMPCPP-FtsZ to be 160 ± 20.[1] Thus, we estimate an upper limit for the radius of gyration of a cyclic oligomer according to

$$R_G \approx \frac{\frac{M}{M_1} \times d}{2\pi} \quad (16)$$

rendering R_G values of ≈915 ± 180 and ≈1270 ± 160 Å for the GTP and GMPCPP polymers, respectively. Because any real cyclic oligomer is unlikely to be precisely circular and planar, its radius of gyration will be somewhat smaller, and therefore, the upper limit estimates presented here are consistent with the estimates of R_G obtained from the model-free interpretation of multiangle light scattering presented above.

DISCUSSION

In this work, we present a modification of a previously proposed linear growth–cyclization model for self-association of FtsZ in the presence of GTP and Mg,[2] which allows for a distinction to be made between the equilibrium association constant for dimer formation and that for subsequent addition of monomer to oligomer, as suggested by Huecas et al.[3] We have demonstrated that this model, using parameter values leading to estimates of oligomer size obtained from measurement of sedimentation and diffusion coefficients,[1] can account quantitatively for the results of extensive measurements of the concentration dependence of both 90° and multiangle light scattering of solutions of FtsZ in the presence of both GTP and the GTP analogue GMPCPP in the presence of various concentrations of Mg. Moreover, the size distributions of species calculated as a function of total protein concentration plotted in Figure 3A–C, calculated using the nucleated isodesmic–cyclization model with parameters obtained by fitting this model to the light scattering data, bear a strong qualitative resemblance to the distributions of sedimentation coefficients previously reported (Figures 1 and 2 in ref 1). In a 1 g/L FtsZ solution containing GTP/RS and 100 μM Mg, significant quantities of both low-molecular weight (slowly sedimenting) and high-molecular weight (rapidly sedimenting) species are present, while in the presence of 5 mM Mg, only a high-molecular weight (rapidly sedimenting) species is present, with a sedimentation coefficient roughly 50% larger than that at 100 μM Mg. In a 0.5 g/L FtsZ solution containing GMPCPP and 5 mM Mg, only a rapidly sedimenting distribution is observed, with a sedimentation coefficient roughly 50% larger than that observed in the solution of FtsZ, GTP/RS, and 5 mM Mg at a concentration of 1 g/L.

The model fitting exercise described in this work is not meant to provide physically realistic parameter values, because the models considered are semiempirical and highly simplified. However, the fact that this model is able to fit a large body of data to within experimental error, whereas existing models for self-association that do not allow for cyclization cannot fit the data even qualitatively, suggests that cyclization plays an essential role in FtsZ self-assembly under the conditions of the experiments described in ref 1. It further demonstrates that a nonequilibrium steady-state model based upon the kinetics of GTP hydrolysis and GTP–GDP exchange is not required to account for the various observations reported in ref 1, since the concentration-dependent behavior indicating cyclization is even more marked in the systems containing GMPCPP, exhibiting little or no nucleotide hydrolysis, than in those containing GTP. Additionally, the multiangle light scattering data do not seem to be compatible with a value of the initial equilibrium constant for dimerization that is smaller

than ~20% of the value of the equilibrium constant for subsequent addition of monomer to growing protofibril, indicating that a true dimer nucleation mechanism[3] is improbable.

The hypothesis of cyclization as a means for providing oligomer stability has been criticized on the grounds that cyclic oligomers do not appear frequently in electron micrographs prepared under different experimental conditions (reviewed in refs 8 and 9). As it is known that the self-assembly of FtsZ depends sensitively upon solution conditions,[8,9] and that the structure of aggregates observed in electron micrographs may depend sensitively upon the method of sample preparation,[10] we do not feel that such comparisons provide a sound basis for rejection of the cyclization hypothesis. If any comparisons between the results of solution studies and the results of solid-state imaging procedures are to be made, the images to be cited should be those of samples prepared from the same solutions on which the solution studies were conducted. One cryo-EM study, a technique that reduces the complication of an underlying substrate by imaging protofilaments suspended in ice over holes in the carbon, although showing that a number of the polymers were indeed curved, found only a small fraction of circular polymers.[3] However, electron microscopic images prepared from the same solutions studied by Monterroso et al.[1] do show a large abundance of curved and cyclic fibrils (Figure S2 of the Supporting Information). Moreover, recent images of samples prepared from the solutions studied in ref 1, obtained by atomic force microscopy,[11] show an abundance of a narrow size distribution of cyclic oligomers of approximately the size predicted by the best fit of the cyclization model proposed here to the combined solution data of ref 1. Finally, in a manner independent of particulars of the model, the estimate of the radius of gyration calculated from the angular dependence of light scattering is in reasonable agreement with that estimated for a cyclic protofibril and qualitatively inconsistent with estimates of the radius of gyration of either a compact oligomer or linear protofibril of equal mass.

A second objection to the cyclization hypothesis raised by Erickson[12] is that the high stability of the hypothetical closed cyclic intermediate is inconsistent with the results of steady-state Förster resonance energy transfer (FRET) experiments interpreted as being indicative of rapid subunit exchange kinetics. The experiments of Erickson and co-workers were conducted with polymers of mutated FtsZ labeled with hydrophobic fluorophores. We believe that the FRET results reported by Erickson may reflect changes in polymer stability and structure (for example, intrinsic curvature and tendency to bundle) arising from mutation and the introduction of fluorophores as well as subunit exchange. In the absence of direct measurement of the extent of polymerization (such as those reported here) and possible changes in the extent of polymerization accompanying Erickson's mixing experiments, FRET measurements alone are not susceptible to unambiguous interpretation.

Fragmentation certainly can limit the size of fibrillar oligomers but by itself cannot elicit a highly concerted formation of a narrow distribution of favored polymers in a manner resembling a phase transition, as we observe here. The sedimentation velocity results recently reported[1] and the predictions of the best-fit model presented here (Figure 3A– C) clearly indicate that, at equilibrium, there is no significant amount of material existing as oligomers intermediate between a low-molecular weight distribution consisting mainly of monomers and dimers and a narrow distribution of high-molecular weight oligomeric species. The major consequence of fragmentation and annealing of fibrils would be acceleration of the approach to equilibrium. The rapid exchange of FtsZ subunits when mixing donor-labeled and acceptor-labeled FtsZ fibrils in the FRET experiments reported by Erickson and co-workers[12] does not require the disappearance of fibrils, merely transient breakage and closure along the length of a fibril. The essential point is that without a mechanism for formation of a discrete oligomer or narrow molecular weight distribution of

oligomers in a highly cooperative fashion (for example, cyclization), nucleation and fragmentation alone will not account for the data.

We do not attribute physiological significance to the presumed cyclic intermediates, because the system studied here is highly simplified and lacks the companion proteins and surfaces required to assemble the septal ring in vivo. However, we believe that the size of the stable oligomers represents a minimum in the dependence of the free energy of loop closure upon filament size, and may thus be a useful indicator of the natural tendency of FtsZ fibrils to flex or curve under a given set of experimental conditions in solution. In this respect, the characterization of FtsZ solution behavior provides information that will ultimately be integrated into more complex schemes describing systems containing the additional elements mentioned above. We speculate that the very high values of ln $K_{max}{}^{c}$ required to fit the data with the nucleated isodesmic–cyclation model may reflect a mechanism of loop closure that involves the formation of several simultaneous side-to-side contacts between FtsZ molecules at fiber termini rather than a single end-to-end contact. If such side-to-side contacts can be detected experimentally via careful analysis of high-resolution images of cyclic fibrils, the generalization of our model would be warranted.

Finally, we must emphasize that although this model does not explicitly invoke nucleotide hydrolysis or exchange, such processes will influence the magnitude of the apparent equilibrium constants appearing in the model. However, any attempt to explicitly include these effects (see, for example, ref 13) will inevitably result in a proliferation of adjustable parameters, and we have shown that additional parameters are not required to account for the data considered here and in ref 1.

Supplementary Material

Refer to Web version on PubMed Central for supplementary material.

Acknowledgments

Funding

This work was supported by the Spanish Ministerio de Ciencia e Innovación through Grants BIO2008-04478-C03 and BIO2011-28941-C03-03, by the European Commission through Contract HEALTH-F3-2009-223432, by the Human Frontiers Science Program through Grant RGP0050/2010-C102, and by the Comunidad de Madrid through Grant S-BIO-0260/2006 to G.R. B.M. is a JAE postdoctoral associate from the European Social Fund and the Spanish Consejo Superior de Investigaciones Científıcas (CSIC). The research of A.P.M. is supported by the Intramural Research Program of the National Institute of Diabetes and Digestive and Kidney Diseases.

We thank I. V. Surovtsev (Texas A&M University, College Station, TX) for useful discussions and comments.

ABBREVIATIONS

GTP/RS	GTP and GTP regeneration system
GMPCPP	guanosine 5-[(α,β)-methyleno]triphosphate, sodium salt
GTP-FtsZ and GMPCPP-FtsZ polymers	polymers of FtsZ in which assembly was triggered by GTP and GMPCPP, respectively

REFERENCES

1. Monterroso B, Ahijado-Guzman R, Reija B, Alfonso C, Zorrilla S, Minton AP, Rivas G. Mg^{2+}-linked FtsZ self-assembly in the presence of GTP or a GTP analog involves the concerted formation

of a narrow distribution of oligomeric species. Biochemistry. 2012; 51:4541–4550. [PubMed: 22568594]

2. González JM, Vélez M, Jiménez M, Alfonso C, Schuck P, Mingorance J, Vicente M, Minton AP, Rivas G. Cooperative behavior of *Escherichia coli* cell-division protein FtsZ assembly involves the preferential cyclization of long single-stranded fibrils. Proc. Natl. Acad. Sci. U.SA. 2005; 102:1895–1900.
3. Huecas S, Llorca O, Boskovic J, Martín-Benito J, Valpuesta JM, Andreu JM. Energetics and geometry of FtsZ polymers: Nucleated self-assembly of single protofilaments. Biophys. J. 2008; 94:1796–1806. [PubMed: 18024502]
4. Dajkovic A, Lutkenhaus J. Z ring as executor of bacterial cell division. J. Mol. Microbiol. Biotechnol. 2006; 11:140–151. [PubMed: 16983191]
5. Lan G, Dajkovic A, Wirtz D, Sun SX. Polymerization and bundling kinetics of FtsZ filaments. Biophys. J. 2008; 95:4045–4056. [PubMed: 18621825]
6. Miraldi ER, Thomas PJ, Romberg L. Allosteric models for cooperative polymerization of linear polymers. Biophys. J. 2008; 95:2470–2486. [PubMed: 18502809]
7. Tanford, C. Physical chemistry of macromolecules. New York: John Wiley & Sons; 1961.
8. Erickson HP, Anderson DE, Osawa M. FtsZ in bacterial cytokinesis: Cytoskeleton and force generator all in one. Microbiol. Mol. Biol. Rev. 2010; 74:504–528. [PubMed: 21119015]
9. Mingorance J, Rivas G, Vélez M, Gómez-Puertas P, Vicente M. Strong FtsZ is with the force: Mechanisms to constrict bacteria. Trends Microbiol. 2010; 18:348–356. [PubMed: 20598544]
10. Hou S, Wieczorek SA, Kaminski TS, Ziebacz N, Tabaka M, Sorto NA, Foss MH, Shaw JT, Thanbichler M, Weibel DB, Nieznanski K, Holyst R, Garstecki P. Characterization of caulobacter crescentus FtsZ using dynamic light scattering. J. Biol. Chem. 2012; 287:23878–23886. [PubMed: 22573335]
11. Mateos-Gil P, Paez A, Horger I, Rivas G, Vicente M, Tarazona P, Velez M. Depolymerization dynamics of individual filaments of bacterial cytoskeletal protein FtsZ. Proc. Natl. Acad. SciU.SA. 2012; 109:8133–8138.
12. Erickson HP. Modeling the physics of FtsZ assembly and force generation. Proc. Natl. Acad. SciU.SA. 2009; 106:9238–9243.
13. Surovtsev IV, Morgan JJ, Lindahl PA. Kinetic Modeling of the Assembly, Dynamic Steady State, and Contraction of the FtsZ Ring in Prokaryotic Cytokinesis. PLoS Comput. Biol. 2008; 4:e1000102. [PubMed: 18604268]

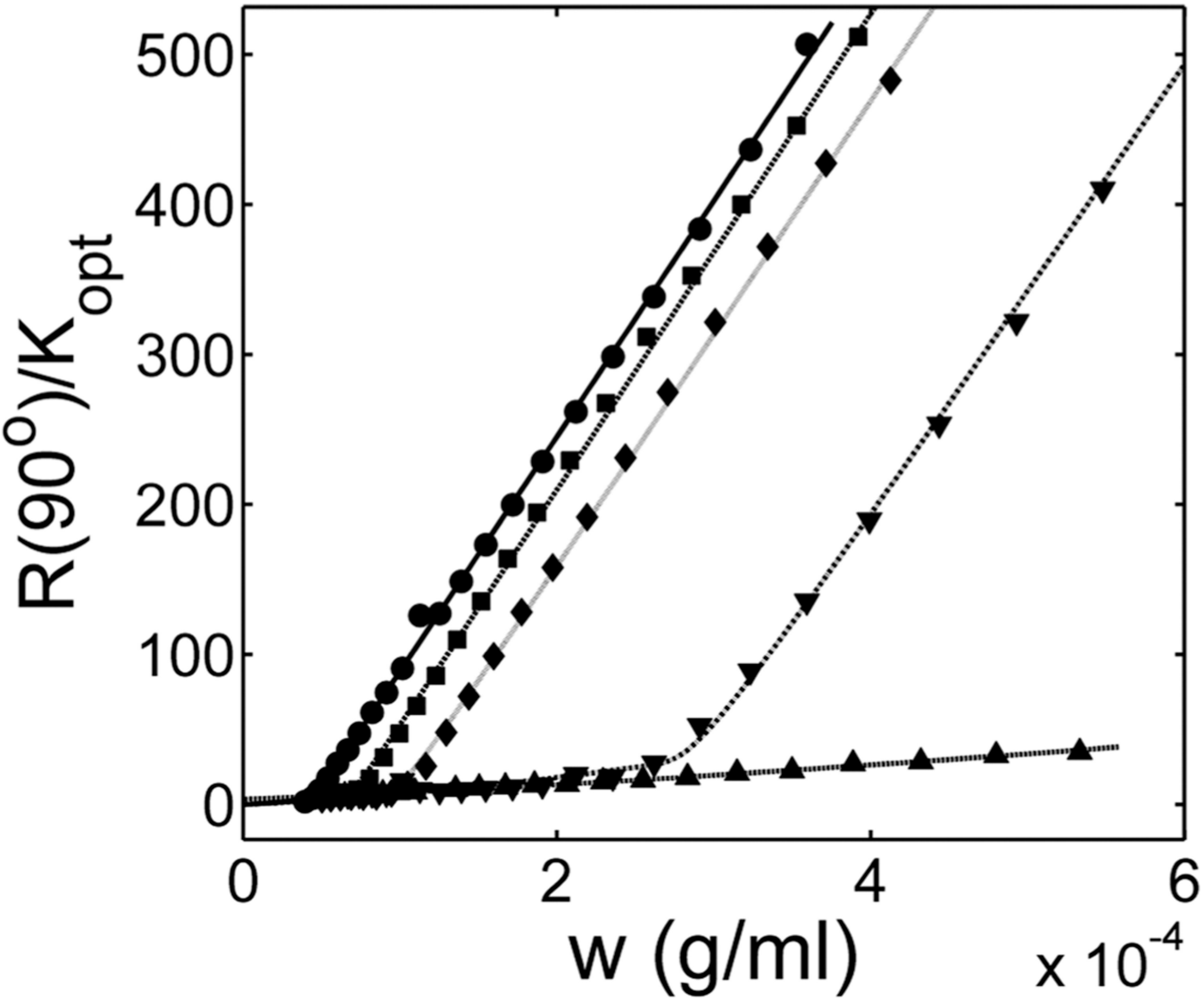

Figure 1.

90° scattering intensity of FtsZ solutions in the presence of GMPCPP and various Mg concentrations: (▲) EDTA, (▼) 20 μM Mg, (◆) 50 μM Mg, (■) 100 μM Mg, and (●) 5 mM Mg. Curves calculated using eqs 4–11 with i_{max} fixed to 190 in accordance with multiangle SLS analysis and Svedberg calculation, Ξ fixed to 3.5 in accordance with results of multiangle SLS analysis, and best-fit values of parameters listed in Table 1.

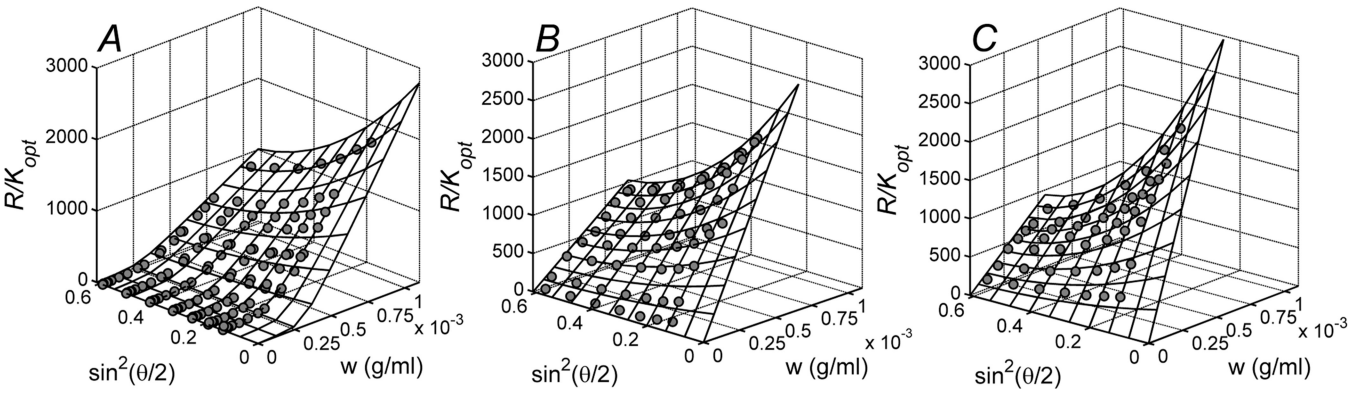

Figure 2.

Scattering intensity of FtsZ solutions in the presence of GTP/RS with 100 μM Mg (A), GTP/RS with 5 mM Mg (B), and GMPCPP with 5 mM Mg (C), plotted as a function of protein concentration w and $\sin^2(\theta/2)$. Also plotted are the concentration and angle dependencies calculated using the nucleated isodesmic−cyclization model of eqs 4–10 and 12 together with the best-fit parameter values listed in Table 2.

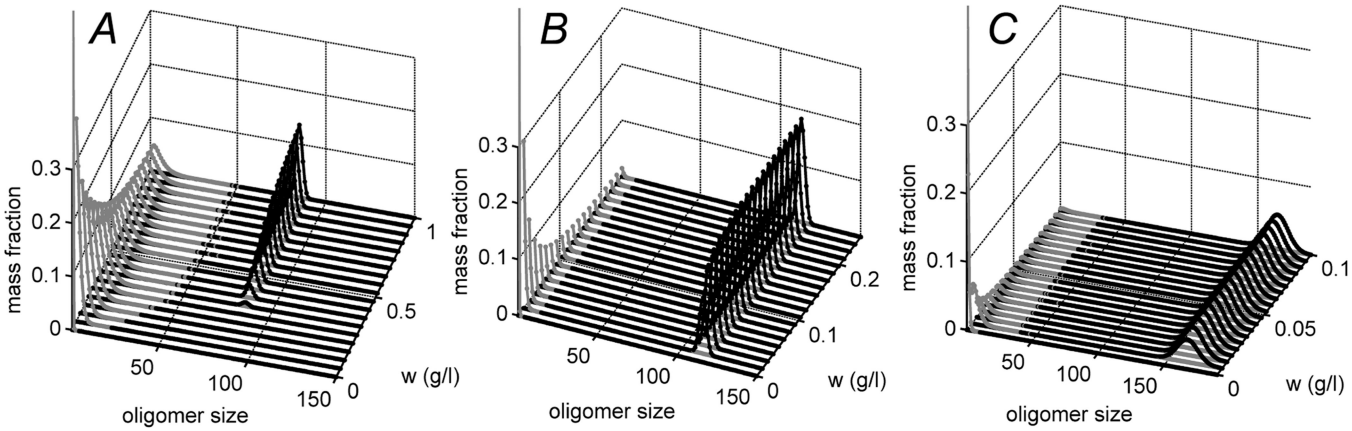

Figure 3.

Fractional abundance of oligomeric species, plotted as a function of oligomer size and total protein concentration, calculated using the nucleated isodesmic–cyclization model of eqs 4–10 for each of the three sets of experimental conditions described in the legend of Figure 2, using the best-fit parameter values listed in Table 2. Gray for linear oligomers and black for cyclic oligomers.

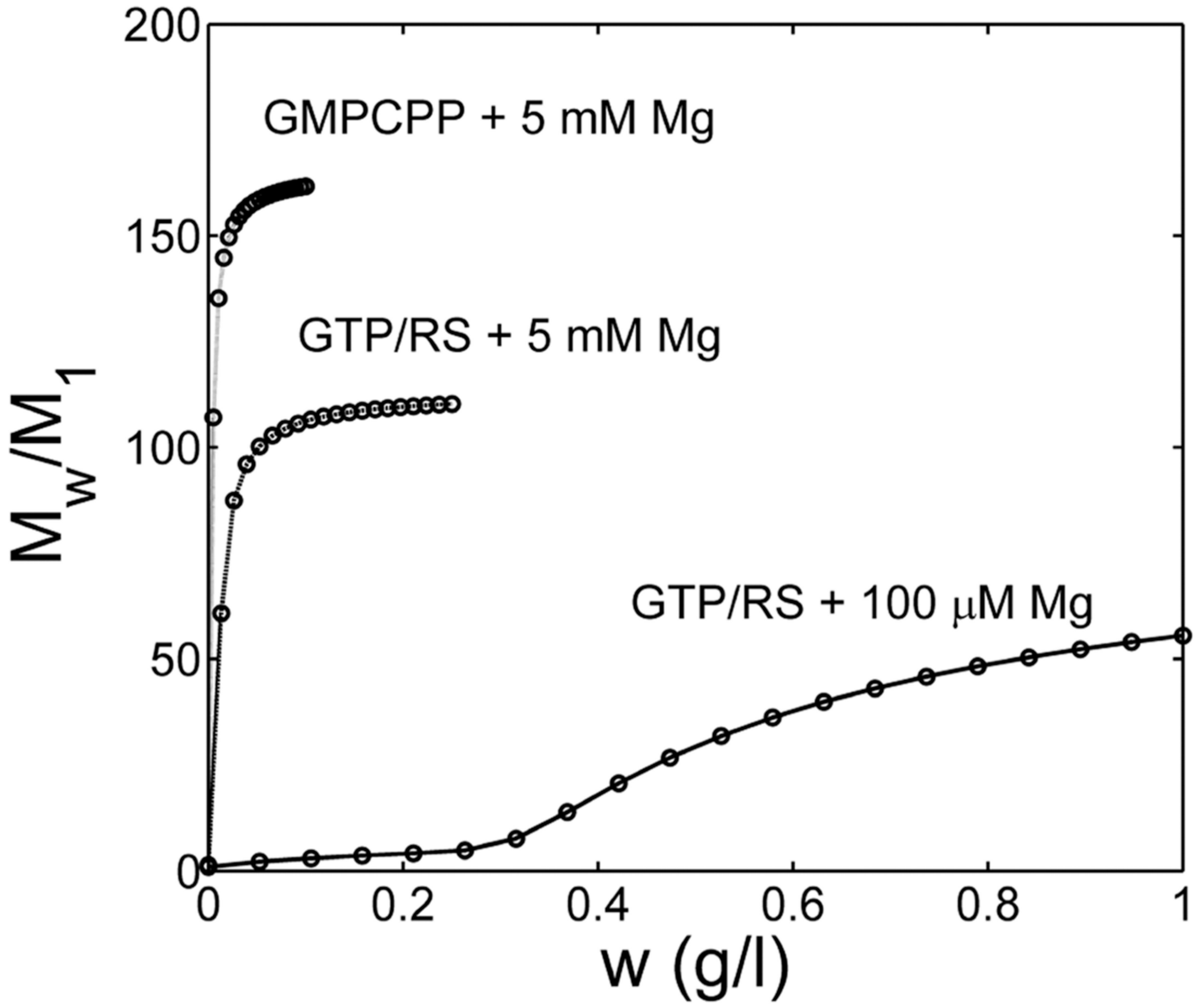

Figure 4.

Weight-average molecular weight of protein, plotted as a function of total protein concentration, calculated using the nucleated isodesmic–cyclization model of eqs 4–10 for each of the three sets of experimental conditions described in the legend of Figure 2, using the best-fit parameter values listed in Table 2.

Table 1

Best-Fit Values of Log K and α in eqs 4–11 Used To Model the Concentration Dependence of 90° Light Scattering Data Measured in FtsZ Solutions Containing GMPCPP and Various Concentrations of Mg (plotted in Figure 1)[a]

[Mg]	log K	α
0 (EDTA)	4.4	1
20 μM	5.3	1.0–1.1
50 μM	5.8	1.0–1.1
100 μM	5.8–6.1	1.0–1.2
5 mM	7.3–7.4	1.0–1.2

[a]The value of ln $K_{max}{}^{c}$ is assumed to be indeterminately large, except in the EDTA solution, where it is assumed to be indeterminately small (i.e., cyclization is undetectable). The values of i_{max}, $\sigma_{i,max}$, and Ξ are constrained to 190, 11, and 3.5, respectively, for consistency with values used to fit the multiangle light scattering data obtained in GMPCPP and 5 mM Mg (see Table 2).

Table 2

Best-Fit Values of Floating Parameters in eqs 4–10 and 12 Used To Model Data Plotted in Figure 2A−C[a]

solution composition	log *K*	α[b]	i_{max}	$\sigma_{i,max}$
GTP/RS with 100 μM Mg	5.7 ± 0.2	0.9[b]	88 ± 7	2.8 ± 0.2
GTP/RS with 5 mM Mg	6.3	0.9[b]	130 ± 20	3.0
GMPCPP with 5 mM Mg	9 ± 1	0.9[b]	190 ± 20	11 ± 1

[a]Only those parameter values that are reasonably well constrained by the data are shown. As described in the text, the values of α and i_{max} may not be determined individually, but the mutually dependent pairs of values plotted in Figure S1 of the Supporting Information may be determined. In all cases, the best-fit value of ln K_{max}[c] exceeds 20 and may be regarded as indeterminately large.

[b]The value of α was that used to calculate the functions plotted in Figure 3A–C. This calculated function is indistinguishable from that calculated using other {α,i_{max}} pairs plotted in Figure S1 of the Supporting Information.